



**NORSAR Scientific Report No. 1-2003**

# **Semiannual Technical Summary**

**1 July - 31 December 2002**

**Frode Ringdal (ed.)**

**Kjeller, February 2003**

## 6 Summary of Technical Reports / Papers Published

### 6.1 Upgrading the ARCES (PS 28) on-line data processing system

#### 6.1.1 Introduction

The main part of the detector recipe for the ARCES array has not been modified since its installation in 1989 (Fyen, 1989). The only major change was an extension with the inclusion of more horizontal beams in 1999 (Kværna et al., 1999) after the sensitivity of these beams for local and regional S phases had been demonstrated in an earlier study (Schweitzer, 1994). However, the detector recipe, as installed in 1989, was restricted by the limited computer capabilities of at that time. It consisted of 76 beams; 66 coherent beams with slowness parameters for regional P onsets, and 10 incoherent beams of narrow-band pre-filtered data for vertical (6) and horizontal (4) components. The change in April 1999 was the addition of 108 new beams; 36 beams of rotated transverse components, 36 beams of rotated radial components, and 36 incoherent beams of horizontal components for an apparent velocity of 4 km/s and various backazimuths. Fig. 6.1.1 shows the slowness distribution of this ARCES beam set. The distribution of red points represent the slowness values used to calculate the different beams as function of ray parameter in [s/deg] and backazimuth in [deg]. Many of the shown slowness values were used several times but for different bandpass filters. All incoherent beams using the vertical components were calculated with an infinite apparent velocity, which places them all in the center of the slowness space. The radii of the blue circles are at 4.4, 13.9, 18.5, and 27.8 s/deg, which corresponds with apparent velocities of P waves from the core-mantle boundary, Pn waves of 8, Pg waves of 6, and regional S waves of 4 km/s, respectively.

However, these detection beams do not cover all interesting parts of the slowness space and after some P onsets, for analysts clearly visible, were not detected by this automatic detector recipe, a principle restructuring of the detector recipe for ARCES data was considered.

#### 6.1.2 The new beam table for ARCES

Since computer capabilities have increased dramatically during the last decade, the first decision for a new ARCES detector recipe was to increase the total number of beams to 573, of which only 13 are incoherent beams. Table 6.1.1 lists the whole new beam set for ARCES. The number of incoherent beams, in particular of horizontal components, was reduced because the small number of only four 3C sites results in a relatively high sensitivity of such beams to disturbances and noise at only one site. This reduction is compensated for by a new set of coherent vertical beams using S-phase typical apparent velocities. Fig. 6.1.2 shows the slowness distribution (ray parameters and backazimuths) of the new beam set. Note that beams are now calculated down to an apparent velocity of 2.5 km/s (or 44.5 s/deg), which resolves much better the numerous Rg-type onsets from local events. In addition, the beams for detecting P onsets are much more evenly distributed in the ray-parameter space of regional and teleseismic P phases up to apparent velocities of lower most-mantle P waves (~20 km/s). To detect PKP onsets, still only beams with an infinite apparent velocity are used. Since the installation of ARCES in 1987, some events had been observed from the Novaya Zemlya area. Therefore, mean observed backazimuth and apparent velocity values could be calculated for this source region. In the new

ARCES beam table, these values are used to calculate five Pn beams and 15 Sn beams in particular sensitive for this source region of interest.

### 6.1.3 Performance of the new ARCES detector recipe

Because of the larger number of beams and the better coverage of the slowness space, the new detector recipe led to a dramatic increase in the number of detections. The new detector recipe was tested over several months in parallel with the original on-line data processing at NORSAR. In the period between 8 August (DOY 220) and 31 October 2002 (DOY 304), the number of detections increased by about 42.3% from 54488 to 77519 detections. In particular, the number of S and Rg onsets increased. As for other arrays, the array-transfer function of the ARCES array is not perfect (see for example, Schweitzer et al., 2002) and a seismic signal will trigger on many different beams. In such cases, the detector processor as developed at NORSAR (Fyen 1989; 2001) chooses the beam which has the best relative signal-to-noise ratio (SNR) that means the highest ratio SNR to predefined detection threshold of the beam. In the detector-result lists the beam names are reported and thereby all beam parameters.

For the 54488 detections with the old detection recipe, 152 of the 184 implemented beams were reported as detecting, of which 70.8% (38571) of the detections were made with coherent and 29.2% (15917) with incoherent beams. The distribution for the new beam deployment is different; during the 84 days test period, 564 of the 573 defined detecting beams (or 98.4%) were the defining beam with best SNR on at least one occasion and only the small number of 2717 (or 3.5%) of all detections were found with incoherent beams. That detection-time estimates on coherent beams are more reliable than on incoherent beams is obvious, consequently the whole automatic parameter extraction by fk-analysis will be more stable for such detected onsets.

From former studies (Schweitzer, 1994; 1997; 1998), it is known how important it is to choose an optimum time-window definition for the automatic fk-analysis. After changing the detector recipe for ARCES, the positioning and length of the time window for the automatic fk-analysis was also modified. For the new ARCES processing, up to eight different time windows are tested for each detection and the one chosen is that which gives the best quality value (i.e., the highest signal coherence) for the fk-analysis. In cases where the original detection was made on one of the horizontal component beams, the fk-analysis is initially performed on the vertical components. A subsequent fk-result is performed on the horizontal components only in cases where the vertical component fk-analysis result displays very low coherence. The later fk-result will then of course be less reliable (note; ARCES has only four 3C sites!) and will only be accepted in the case of measured apparent velocities belonging to S- or Rg-type onsets.

All phase identifications are based on these slowness measurements done during the automatic data processing. Table 6.1.2 gives some additional information about the differences between the old and the new beam recipes with respect to the different phase types. The number of detected phases increases for all types of detections apart from a small decrease in P- and PKP-type detections. This reduction is understandable given the better coverage of the slowness space (compare Fig. 6.1.1 with Fig. 6.1.2); slower phases are much less often detected and wrongly interpreted as teleseismic onsets and many regional P onsets are now much better detected by the Pn- and Pg-type beams and consequently also more robustly analyzed.

#### 6.1.4 Event locations

The results for the automatic measurement of onset times, apparent velocities, backazimuths, amplitudes and dominant signal frequencies are used in a later step of NORSAR's automatic data processing for single array (RONAPP, Mykkeltveit and Bungum, 1984) and multi array (GBF, Ringdal and Kværna, 1989) locations. The described modifications to the recipes for detector and fk-analysis should also improve these location results.

Between 8 August (DOY 220) and 31 October 2002 (DOY 304), the number of located events using the RONAPP algorithm increased by about 23.9% from 3072 to 3806 located events. The geographical distribution of the two event sets is shown in Fig. 6.1.3 and Fig. 6.1.4. For orientation on both maps, circles of 500 km and 1000 km distance around ARCES are shown. It is known that single array locations from small aperture regional arrays show some scatter. To show only the most robust solutions, the located events were binned on both figures in 1000 km<sup>2</sup> large areas and the number of events per bin is shown in a color coded scale. No bin containing only one event is shown. The number of bins is 213 for the old and 255 for the new processing results. However, the number of bins containing only one event also increased from 820 to 1011; i.e., in both cases about 75% of all bins were hit only once. Most of the events occur inside the 500 km radius around ARCES. The differences between the two maps are not very large. However, the known source areas of mining activities in Kiruna, Malmberg, Khibiny, and in Finland show more events for the new data processing results. This is also true for events on the Mid Atlantic Ridge southwest of Spitsbergen.

The next step in evaluating the new ARCES data processing was in comparing the GBF bulletins produced with the old and new ARCES fk-results. For a period of 58 days (8 August - 5 October 2002), GBF was reprocessed using the new automatic ARCES results. The total number of events located by GBF using the old and the new ARCES data processing is only slightly changed. However, comparing the single locations, some differences become evident. Because not only the fk-results but also the onset time estimations and the total number of ARCES observations changed, the whole GBF bulletin shows many differences, some of them being listed in Table 6.1.3. To compare two such different bulletins, one has to define the criterion that two event locations represent identical seismic events. Because most locations in the GBF bulletins are based on a relatively small number of defining parameters, changing, adding, or removing one of these defining parameters can drastically change the epicenter determination. Therefore, in this study two events were defined as common if the horizontal distance between them is not more than 150 km and if the origin-time difference between these two events is not more than 25 s. Using these rules, both GBF bulletins have 17222 or more than 80% common events. The new GBF results show a systematic shift of locations to better defined events; as also shown in Table 6.1.3, the number of single array solutions decreased by 4.6% from 17145 to 16375 events, and the number of events observed by more than two stations increases by 18.9% from 797 to 948 events.

Events located with observations from at least two stations with a defining P onset and at one of these two stations in addition with a defining S onset are assumed to be relatively well located GBF events. The number of such events increased by 16%. However, 88 of the events from the GBF bulletins created using the old ARCES results do not appear in the GBF bulletins created with the new ARCES results. This can have two reasons; for some events the new ARCES contribution moved the event outside the 150 km and/or 25 s limit or the new ARCES results no longer contribute with observations that the event is just no longer definable. Fig. 6.1.5 shows a

map with all 88 events, which are not longer defined in the GBF bulletins using the new ARCES results. Most of the events are scattered in or around the Barents Sea region.

The same is true for the 186 events Fig. 6.1.6 which are only in the GBF bulletin using the new ARCES results; many of these new events lay in the vicinity of either the ARCES or the SPITS arrays, both arrays with a high number of detections and local or regional events nearby. In these cases, onsets from the other array can by chance easily erroneously be associated to such a one array solution.

### **6.1.5 Conclusions**

The analysis of the new ARCES processing results clearly shows a better adjustment to the observed seismic onsets at the array site. The number of detections increases and on average the seismic phases are detected with a higher SNR. The number of single array event locations is higher and a relative increase in spurious events is not be observed. Comparing the GBF results shows that the number of more reliably defined events increases. This is eventually connected with a slight increase of erroneous defined events (see Fig. 6.1.6). The latter happened in particular in connection with observations of the SPITS array. This point has to be observed and a change of the GBF processing scheme in the case of two-station event locations may be considered in the future.

Because of these overall positive results the new beam set and data processing recipes were installed for NORSAR' s on-line processing of ARCES data from 21 November 2002 (DOY 325) on.

**Johannes Schweitzer**

---

*References*

- Fyen, J. (1989): Improvements and modifications. Semiannual Technical Summary, 1 April 1988 - 30 September 1988, NORSAR Scientific Report **1-89/90**, 30-38.
- Fyen, J. (2001): NORSAR seismic data processing - user guide and command reference. NORSAR (contribution 731), Kjeller, Norway.
- Kværna, T., J. Schweitzer, L. Taylor and F. Ringdal (1999): Monitoring of the European Arctic Using Regional Generalized Beamforming. Semiannual Technical Summary, 1 October 1998 - 31 March 1999, NORSAR Scientific Report **2-98/99**, 78-94.
- Mykkeltveit, S. and H. Bungum (1984): Processing of regional seismic events using data from small-aperture arrays. *Bull. Seism. Soc. Am.* **74**, 2313-2333.
- Ringdal, F. and T. Kværna (1989): A multi-channel processing approach to real time network detection, phase association, and threshold monitoring. *Bull. Seism. Soc. Am.* **79**, 1927-1940.
- Schweitzer, J. (1994): Some improvements of the detector / SigPro-system at NORSAR. Semiannual Technical Summary, 1 October 1993 - 31 March 1994, NORSAR Scientific Report **2-93/94**, 128-139.
- Schweitzer, J. (1997): Recommendations for improvements in the PIDC processing of Matsushiro (MJAR) array data. Semiannual Technical Summary, 1 April - 30 September 1997, NORSAR Scientific Report **1-97/98**, 128-141.
- Schweitzer, J. (1998): Tuning the automatic data processing for the Spitsbergen array (SPITS). Semiannual Technical Summary, 1 April - 30 September 1998, NORSAR Scientific Report **1-98/99**, 110-125.
- Schweitzer, J., J. Fyen, S. Mykkeltveit and T. Kværna (2002): Seismic Arrays. **In:** P. Bormann (ed.) (2002): *New Manual of Seismological Observatory Practice (NMSOP)*, Chapter 9, 52 pp.

**Table 6.1.1. Definition of all beams used in the new configuration of the on-line detector for ARCES. Listed are beam names, applied apparent velocities (VEL), backazimuths (BAZ), bandpass and order (ord) of the Butterworth filters, the detection thresholds (THR), and the beam configurations (CONFIG).**

BEAM NAME	VEL [km/s]	BAZ [°]	FILTER		THR	CONFIG
			bandpass [Hz]	ord		
FA01	99999.9	0.0	0.8 – 2.0	4	3.8	ALL
FA02	99999.9	0.0	0.8 – 2.0	4	3.8	DRING
FA03	99999.9	0.0	0.8 – 2.0	4	3.8	TELEV
FA04	99999.9	0.0	0.8 – 2.0	4	3.8	CRING
FA05	99999.9	0.0	1.0 – 2.5	3	3.8	ALL
FA06	99999.9	0.0	1.0 – 2.5	3	3.8	DRING
FA07	99999.9	0.0	1.0 – 2.5	3	3.8	TELEV
FA08	99999.9	0.0	1.0 – 2.5	3	3.8	CRING
FA09	99999.9	0.0	3.0 – 5.0	3	3.8	ALL
FA10	99999.9	0.0	3.0 – 5.0	3	3.8	DRING
FA11	99999.9	0.0	3.0 – 5.0	3	3.8	TELEV
FA12	99999.9	0.0	3.0 – 5.0	3	3.8	CRING
FB01 – FB06	18.0	0 60 120 180 240 300	1.0 – 2.5	3	3.8	TELE
FB07 – FB12	18.0	0 60 120 180 240 300	2.5 – 4.0	3	3.8	TELE
FB09 – FB18	18.0	0 60 120 180 240 300	3.5 – 5.5	3	3.8	TELE
FB19 – FB24	20.0	30 90 150 210 270 330	0.8 – 2.0	4	3.8	ALL
FB25 – FB30	20.0	30 90 150 210 270 330	1.0 – 2.0	3	3.8	ALL
FB31 – FB36	20.0	30 90 150 210 270 330	3.0 – 5.0	3	3.8	ALL
FC01 – FC06	16.0	0 60 120 180 240 300	0.8 – 2.0	4	3.8	ALL
FC07 – FC12	16.0	0 60 120 180 240 300	1.0 – 2.5	3	3.8	ALL
FC13 – FC18	16.0	0 60 120 180 240 300	3.0 – 5.0	3	3.8	ALL
FC19 – FC24	14.0	30 90 150 210 270 330	1.0 – 2.5	3	3.8	DRING
FC25 – FC30	14.0	30 90 150 210 270 330	2.5 – 4.0	3	3.8	DRING
FC31 – FC36	14.0	30 90 150 210 270 330	3.5 – 5.5	3	3.8	DRING
FD01 – FD08	13.0	0 45 90 135 180 225 270 315	1.5 – 3.0	3	3.8	ALL
FD13 – FD20	13.0	0 45 90 135 180 225 270 315	3.0 – 5.0	3	3.8	ALL
FD25 – FD32	13.0	0 45 90 135 180 225 270 315	4.0 – 8.0	3	3.8	ALL
FD37 – FD44	11.0	22.5 67.5 112.5 202.5 247.5 292.5 337.5	2.0 – 3.5	3	3.8	INTER
FD49 – FD56	11.0	22.5 67.5 112.5 202.5 247.5 292.5 337.5	3.5 – 5.5	3	3.8	INTER
FD61 – FD68	11.0	22.5 67.5 112.5 202.5 247.5 292.5 337.5	5.0 – 10.0	3	3.8	INTER
FE01 – FE12	10.0	0 30 60 90 120 150 180 210 240 270 300 330	2.0 – 3.5	3	3.8	ALL
FE13 – FE24	10.0	0 30 60 90 120 150 180 210 240 270 300 330	3.0 – 5.0	3	3.8	ALL
FE25 – FE36	10.0	0 30 60 90 120 150 180 210 240 270 300 330	4.0 – 8.0	3	3.8	ALL
FE37 – FE48	9.0	0 30 60 90 120 150 180 210 240 270 300 330	2.5 – 4.0	3	3.8	CRING
FE49 – FE60	9.0	0 30 60 90 120 150 180 210 240 270 300 330	3.5 – 5.5	3	3.8	CRING
FE61 – FE72	9.0	0 30 60 90 120 150 180 210 240 270 300 330	5.0 – 10.0	3	3.8	CRING
FF01 – FF12	8.5	0 30 60 90 120 150 180 210 240 270 300 330	2.0 – 3.5	3	3.8	ALL
FF13 – FF24	8.5	0 30 60 90 120 150 180 210 240 270 300 330	3.0 – 5.0	3	3.8	ALL
FF25 – FF36	8.5	0 30 60 90 120 150 180 210 240 270 300 330	4.0 – 8.0	3	3.8	ALL
FF37 – FF48	7.5	0 30 60 90 120 150 180 210 240 270 300 330	2.5 – 4.0	3	3.8	CRING
FF49 – FF60	7.5	0 30 60 90 120 150 180 210 240 270 300 330	3.5 – 5.5	3	3.8	CRING
FF61 – FF72	7.5	0 30 60 90 120 150 180 210 240 270 300 330	5.0 – 10.0	3	3.8	CRING
FG01 – FG12	6.5	0 30 60 90 120 150 180 210 240 270 300 330	2.0 – 3.5	3	3.8	ALL
FG13 – FG24	6.5	0 30 60 90 120 150 180 210 240 270 300 330	3.0 – 5.0	3	3.8	ALL
FG25 – FG36	6.5	0 30 60 90 120 150 180 210 240 270 300 330	4.0 – 8.0	3	3.8	ALL
FG37 – FG48	6.0	0 30 60 90 120 150 180 210 240 270 300 330	2.5 – 4.0	3	3.8	CRING
FG49 – FG60	6.0	0 30 60 90 120 150 180 210 240 270 300 330	3.5 – 5.5	3	3.8	CRING
FG61 – FG72	6.0	0 30 60 90 120 150 180 210 240 270 300 330	5.0 – 10.0	3	3.8	CRING
FI01 – FI12	4.5	0 30 60 90 120 150 180 210 240 270 300 330	1.5 – 3.0	3	3.8	ALL
FI13 – FI24	4.5	0 30 60 90 120 150 180 210 240 270 300 330	2.5 – 4.0	3	3.8	ALL
FI25 – FI36	4.5	0 30 60 90 120 150 180 210 240 270 300 330	4.0 – 8.0	3	3.8	ALL
FJ01 – FJ12	3.5	0 30 60 90 120 150 180 210 240 270 300 330	1.5 – 3.0	3	3.8	ALL
FJ13 – FJ24	3.5	0 30 60 90 120 150 180 210 240 270 300 330	2.5 – 4.0	3	3.8	ALL
FJ25 – FJ36	3.5	0 30 60 90 120 150 180 210 240 270 300 330	4.0 – 8.0	3	3.8	ALL
FK01 – FK12	2.5	0 30 60 90 120 150 180 210 240 270 300 330	1.0 – 2.5	3	3.8	ALL
FK13 – FK24	2.5	0 30 60 90 120 150 180 210 240 270 300 330	3.0 – 5.0	3	3.8	ALL

FK25 – FK36	2.5	0 30 60 90 120 150 180 210 240 270 300 330	4.0 – 8.0	3	3.8	ALL
FK37 – FK48	2.5	0 30 60 90 120 150 180 210 240 270 300 330	5.0 – 10.0	3	3.8	BRING
FN01	10.0	64.	1.5 – 3.0	3	3.5	ALL *
FN02	10.0	64	2.5 – 4.0	3	3.5	ALL *
FN03	10.0	64	3.5 – 5.5	3	3.5	ALL *
FN04	10.0	64	5.0 – 10.0	3	3.5	CRING *
FN05	10.0	64	6.0 – 12.0	3	3.5	CRING *
FN06	5.0	58	1.5 – 3.0	3	3.5	ALL *
FN07	5.0	58	2.0 – 3.5	3	3.5	ALL *
FN08	5.0	58	2.5 – 4.0	3	3.5	ALL *
FN09	5.0	58	3.0 – 5.0	3	3.5	ALL *
FN10	5.0	58	4.0 – 8.0	3	3.5	ALL *
FR01 – FR12	4.0	0 30 60 90 120 150 180 210 240 270 300 330	1.0 – 2.0	3	3.8	HR
FR13 – FR24	4.0	0 30 60 90 120 150 180 210 240 270 300 330	3.5 – 5.5	3	3.5	HR
FR25 – FR36	4.0	0 30 60 90 120 150 180 210 240 270 300 330	2.0 – 3.5	3	3.5	HR
FH01 – FH12	4.0	0 30 60 90 120 150 180 210 240 270 300 330	1.0 – 2.0	3	3.8	HT
FH13 – FH24	4.0	0 30 60 90 120 150 180 210 240 270 300 330	3.5 – 5.5	3	3.5	HT
FH25 – FH36	4.0	0 30 60 90 120 150 180 210 240 270 300 330	2.0 – 3.5	3	3.5	HT
FNR1	5.0	58	1.5 – 3.0	3	3.5	HR *
FNR2	5.0	58	2.0 – 3.5	3	3.5	HR *
FNR3	5.0	58	2.5 – 4.5	3	3.5	HR *
FNR4	5.0	58	3.0 – 5.0	3	3.5	HR *
FNR5	5.0	58	4.0 – 8.0	3	3.5	HR *
FNT1	5.0	58	1.5 – 3.0	3	3.5	HT *
FNT2	5.0	58	2.0 – 3.5	3	3.5	HT *
FNT3	5.0	58	2.5 – 4.5	3	3.5	HT *
FNT4	5.0	58	3.0 – 5.0	3	3.5	HT *
FNT5	5.0	58	4.0 – 8.0	3	3.5	HT *
FS13 – FS24	4.0	0 30 60 90 120 150 180 210 240 270 300 330.	1.0 – 2.5	3	3.0	HINC
FV01	99999.9	0.	6.0 – 12.0	3	2.4	VINC

Explanation for the codes used in the column CONFIG:

ALL means all vertical instruments of the ARCES array.

BRING means vertical instruments at the ARCES sites A0, A1, A2, A3, B1, B2, B3, B4, and B5.

CRING means vertical instruments at the ARCES sites A0, B1, B2, B3, B4, B5, C1, C2, C3, C4, C5, C6, and C7

DRING means vertical instruments at the ARCES sites A0, D1, D2, D3, D4, D5, D6, D7, D8, and D9.

HINC means incoherent beam using both horizontal components at the ARCES sites A0, C2, C4, and C7.

HR means radial components rotated from the original horizontal components at the ARCES sites A0, C2, C4, and C7. The rotation angle is identical with the beam azimuth.

HT means transverse components rotated from the original horizontal components at the ARCES sites A0, C2, C4, and C7. The rotation angle is identical with the beam azimuth.

INTER means vertical instruments at the ARCES sites A0, B1, B2, B3, B4, B5, C1, C2, C3, C4, C5, C6, C7, D1, D2, D3, D4, D5, D6, D7, D8, and D9.

TELEV means vertical instruments at the ARCES sites A0, C1, C2, C3, C4, C5, C6, C7, D1, D2, D3, D4, D5, D6, D7, D8, and D9.

VINC means incoherent beam using the vertical components at the ARCES sites A0, C1, C2, C3, C4, C5, C6, and C7.

All beam configurations marked with an star (\*) are beams using the apparent velocities and backazimuths for Pn and Sn phases as observed at ARCES for events in the Novaya Zemlya area.



**Table 6.1.2. Results of the old and new ARCES beam deployment. # gives the number of detections, the percent value is with respect to the total number of detections,  $\overline{\text{SNR}}$  is the mean value of the measured SNR values, 'sum' are all accepted detections after automatic fk-analysis.**

Phase	OLD			NEW		
	#	%	$\overline{\text{SNR}}$	#	%	$\overline{\text{SNR}}$
P / PKP	4176	7.8	12.52	3767	4.9	13.66
Pn / Pg	10563	19.4	9.11	14399	18.6	8.53
S / Sn	8487	15.6	5.08	10906	14.1	5.34
Sg / Lg	14290	26.2	4.64	15488	20.0	5.58
Rg	15003	27.5	6.19	29639	38.2	6.32
sum	52519	96.4	6.68	74199	95.7	6.83
noise/error	1969	3.6	-	3320	4.3	-

**Table 6.1.3. Evaluation of the GBF results one time using the OLD and one time using the NEW automatic fk-results for ARCES. The locations of the events of the table cells with gray background are plotted in Fig. 6.1.5 and Fig. 6.1.6, respectively.**

	Number of events		events occurring	
	OLD	NEW	only in OLD	only in NEW
all events	21433	21462	4211	4240
single station	17145	16374	2790	2231
2 st, 1 st with P + S	789	915	88	186

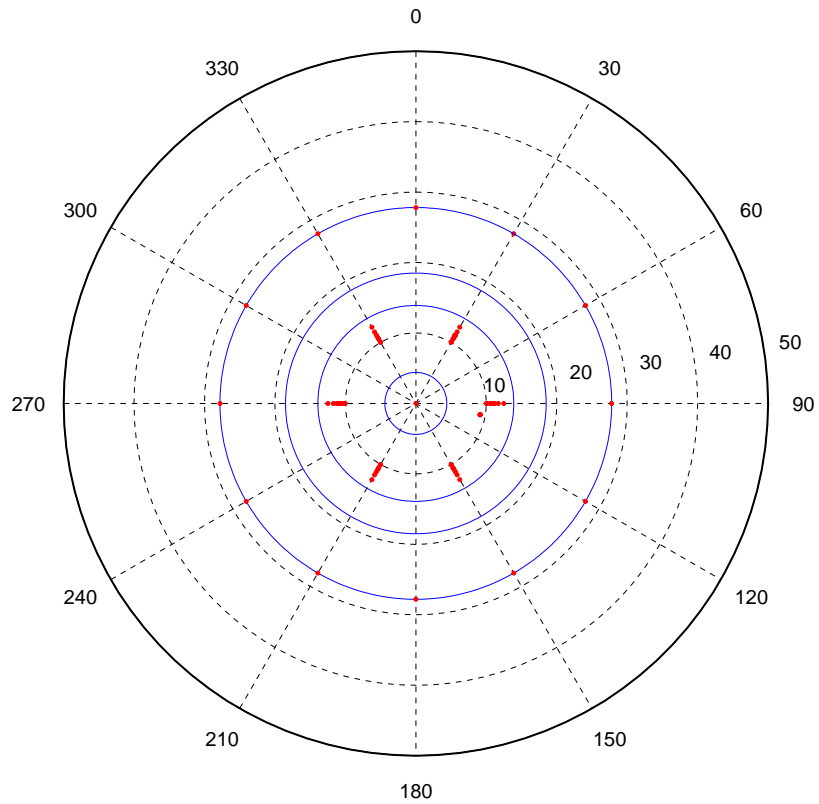


**Fig. 6.1.1.** Coverage of the slowness space by the old ARCES beam deployment (details see text).

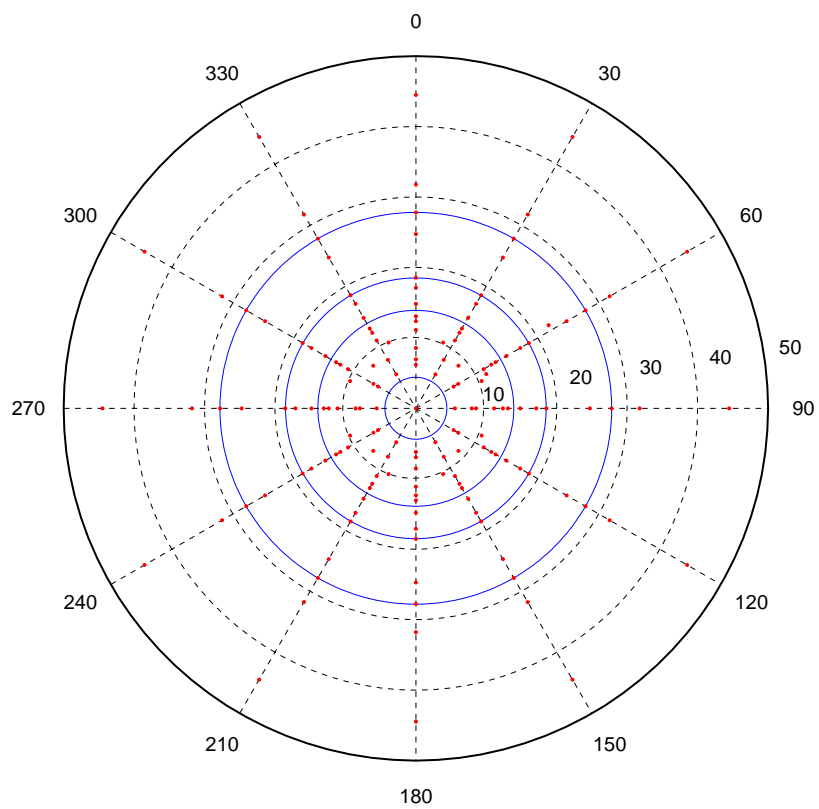


**Fig. 6.1.2.** As Fig. 6.1.1, now for the new ARCES beam deployment.

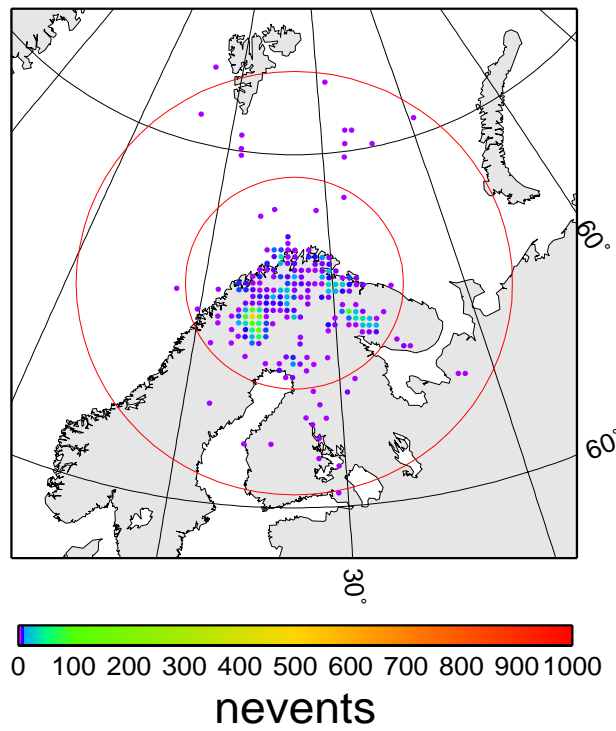


**Fig. 6.1.3.** Seismic events as located by the RONAPP algorithm using the *fk*-results from the old ARCES beam table. Shown are only bins (size 1000 km<sup>2</sup>) with at least 2 events.

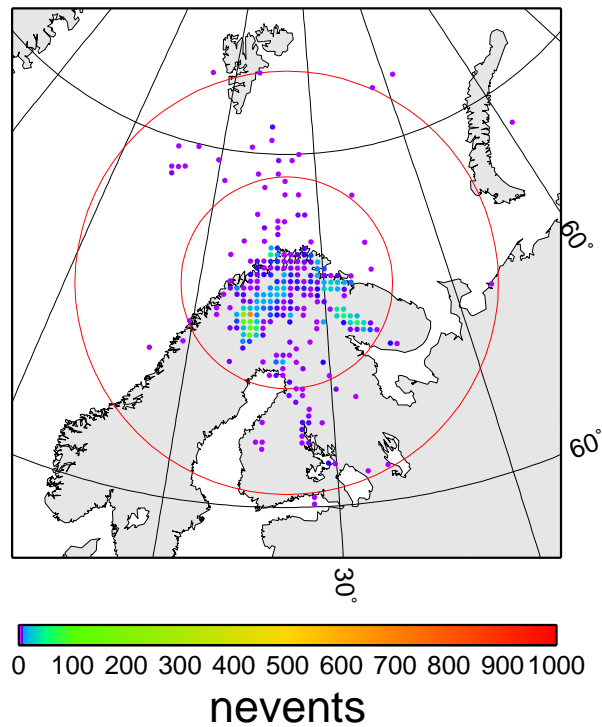


**Fig. 6.1.4.** As Fig. 6.1.3, but the events using the *fk*-results from the new ARCES beam table.

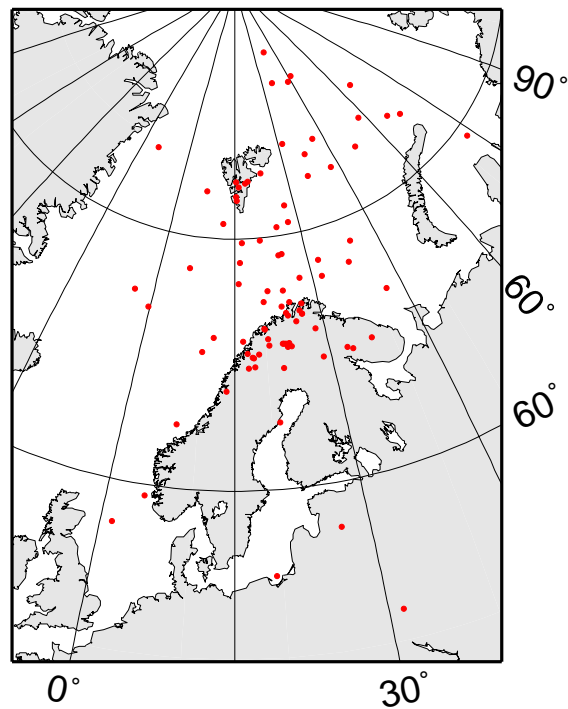


**Fig. 6.1.5.** Events located by GBF with at least 2 *P* onsets at 2 different stations and 1 *P* + 1 *S* onsets as defining observation at one station using the old ARCES processing results; here are only shown the 88 events, which were not in the GBF bulletins using the new ARCES recipes (see Table 6.1.3).

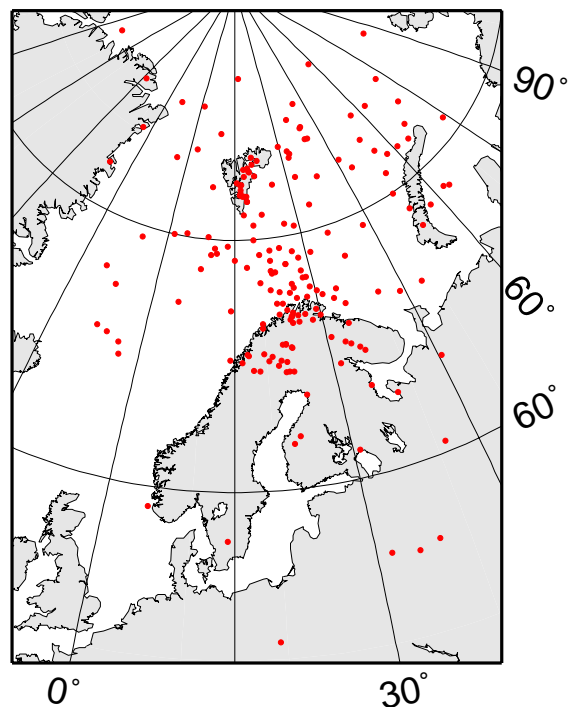


**Fig. 6.1.6.** As Fig. 6.1.5, now showing the 186 events located by the GBF system applying the new ARCES recipes but not located by the old recipes (see Table 6.1.3).

